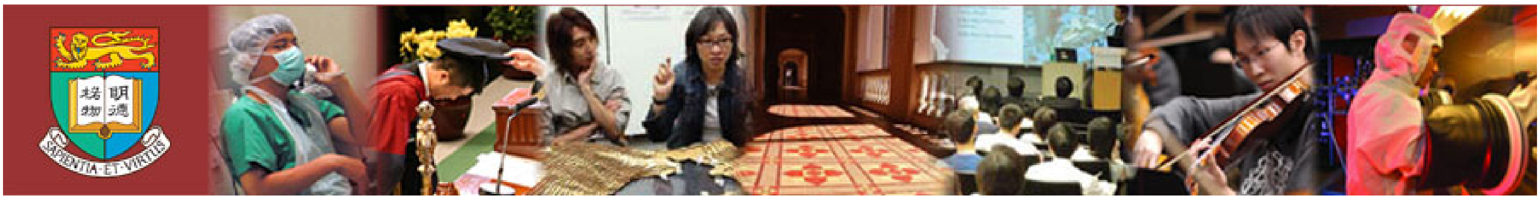

Title	A Single-Layer Compact HF-UHF Dual-Band RFID Tag Antenna
Author(s)	MA, Z; Jiang, L; Xi, J.T.; Ye, T.
Citation	IEEE Antennas and Wireless Propagation Letters, 2012, v. 11, p. 1257-1260
Issued Date	2012
URL	http://hdl.handle.net/10722/185865
Rights	IEEE Antennas and Wireless Propagation Letters. Copyright © IEEE

A Single-Layer Compact HF-UHF Dual-Band RFID Tag Antenna

Zi Long Ma, Li Jun Jiang, *Member, IEEE*, Jingtian Xi, and Terry Tao Ye

***Abstract*—This letter presents a novel dual-band (HF and UHF) radio frequency identification (RFID) tag antenna. Two key challenges are faced: the compact dimension and the impaired bandwidth due to the couplings between two band structures. To enable the implementation of whole design on a credit-card-size single-layer support, a spiral coil along the edges of the card is designed to handle the HF (13.56 MHz) near-field coupling, and the UHF antenna is placed inside the coil instead of outside. Meanwhile, a diagonal symmetric design consisting of two meander lines inside the spiral coil is adopted for UHF band. This structure supports multiple resonance modes around 915 MHz to broaden the working bandwidth under the large inductive circumstance from the HF coil. The proposed antenna is easy for adjustment with ways of handling both coarse tuning and fine-tuning. Its overall dimension is of a credit card size on a single-layer thin substrate. The design methodology and antenna measurement results are both presented and discussed in the letter.**

***Index Terms*—Compact structure, dual-band radio frequency identification (RFID) tag antenna, HF tag antenna, single layer, UHF tag antenna.**

I. Introduction

RADIO frequency identification (RFID), as a fast growing technology in recent years, has been applied in many areas, such as logistics, inventory management and bio-engineering, etc. [1]. To fulfill different kinds of requirements, various communication protocol standards, and operating frequency bands are established. In terms of operating frequency band, HF band is widely applied in short-distance reading applications, such as the campus card system. UHF band is often applied in long-distance reading applications. In addition, the frequency allocations of different countries are quite different. For UHF bands, 866–869 MHz is used in Europe, 902–928 MHz in North and South America, and 950–956 MHz in Japan and some Asian countries [2].

For some special cases, like highway tracking and tolls, both short-distance and long-distance reading are needed. Hence, a single RFID card with dual standards is demanded. From an academic point of view, the research on the dual-band antenna with nearly 70 times frequency difference is also an interesting challenge.

Some research on HF-UHF dual-band antennas has been published in the past few years. Mono feeding port type [3] and dual feeding port type [4]–[8] were discussed. For the dual feeding port type, the spiral coil and meander-line dipole are used as the HF antenna and the UHF antenna, respectively. References [4] and [6] discussed the case when the UHF antenna is placed outside the HF coil. The mutual interaction issue and decoupling issue between UHF and HF antennas are analyzed. In [5] and [7], studies of integrating the UHF antenna inside the coil are presented. Due to the existence of a large inductive coil, its quality factor Q is very high. For serial circuits, $Q = \omega_0 L/R$, and the bandwidth is proportional to $1/Q$. The larger the L, the narrower the bandwidth. Placing the UHF antenna inside the coil can reduce the whole antenna dimension. However, the narrow band becomes an issue to be solved.

In this letter, a novel single-layer dual-band RFID tag antenna is presented. Unlike many existing works, it places the UHF antenna inside the HF coil to enable the compact implementation on a credit-card-size substrate. Therefore, the coupling between HF and UHF antennas causes the Q of the system to be very high at UHF because of the huge parasitic inductance from the HF coil. Hence, the working bandwidth is narrow. To expand the bandwidth, a diagonal symmetric design consisting of two meander lines inside the spiral coil is adopted for the UHF band to support multiple resonance modes around 915 MHz. As a result, both compactness and enough bandwidth are achieved through the proposed design. The design methodology is verified by the measurements including the practical UHF RFID reading range test. It fully demonstrated the feasibility of the proposed idea.

This letter is organized as follows. Section II introduces the antenna's structure and dimensions. Section III gives the design methodology and result analysis of HF and UHF parts, respectively. The antenna's operation principle and impedance matching method are discussed.

II. Antenna Structure

The proposed antenna structure is shown in Fig. 1. It has two feeding ports connecting HF and UHF RFID chips, respectively. The HF antenna is a spiral coil with $W_c = 51.4$ mm, $L_c = 83.6$ mm, $D = 0.4$ mm, and $t_1 = 0.6$ mm. The UHF antenna structure parameters are $W_d = 36$ mm, $L_d = 68$ mm, $D_x = 2.2$ mm, $D_y = 2.2$ mm, $D_1 = 2.3$ mm, $D_2 = 3.8$ mm, $D_3 = 2.5$ mm, $D_4 = 4$ mm, $D_c = 2$ mm, $M_1 = 14$ mm, $M_2 = 26$ mm, $M_3 = 4$ mm, $M_4 = 4$ mm, $M_5 = 6$ mm, $W = 9$ mm, $A = 6$ mm, $B = 6$ mm, $S = 4$ mm, and $t_2 = 1$ mm. Dimensions of each feeding port are $W_p = 2$ mm and $L_p = 2$ mm. It should be noted that the UHF antenna is a diagonal symmetric structure. D_1 and D_2 are different from

Manuscript received September 01, 2012; revised October 15, 2012; accepted October 16, 2012. Date of publication October 19, 2012; date of current version November 19, 2012. This work was supported in part by the Research Grants Council of Hong Kong (GRF 711511 and 713011), HK ITP/026/11LP, HKU Seed Funding (201102160033), and the University Grants Council of Hong Kong under Contract No. AoE/P-04/08.

Z. L. Ma and L. J. Jiang are with the Department of Electrical and Electronic Engineering, University of Hong Kong, Hong Kong (e-mail: zlma@eee.hku.hk; ljiang@eee.hku.hk).

J. Xi and T. T. Ye are with the Hong Kong R&D Centre for Logistics and Supply Chain Management Enabling Technologies, Hong Kong.

Color versions of one or more of the figures in this letter are available online at http://ieeexplore.ieee.org.

Digital Object Identifier 10.1109/LAWP.2012.2225821

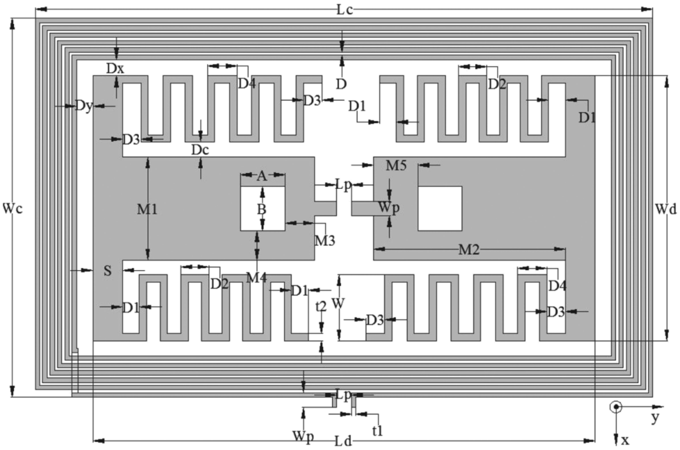

Fig. 1. Proposed antenna structure.

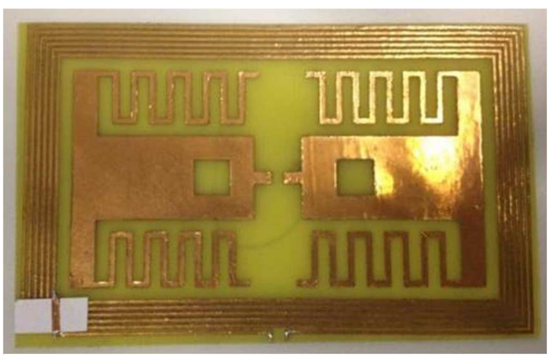

Fig. 2. Photograph of the manufactured design.

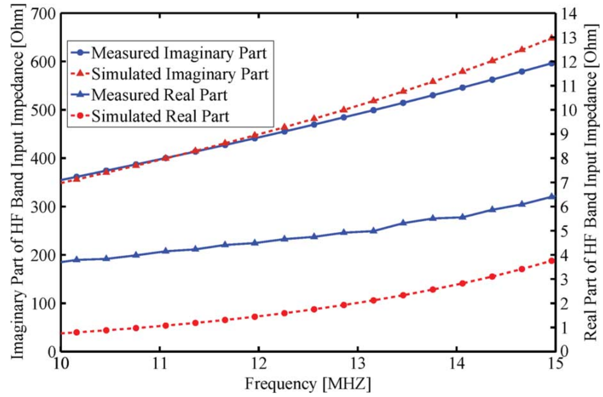

Fig. 3. Measured and simulated HF band input impedance.

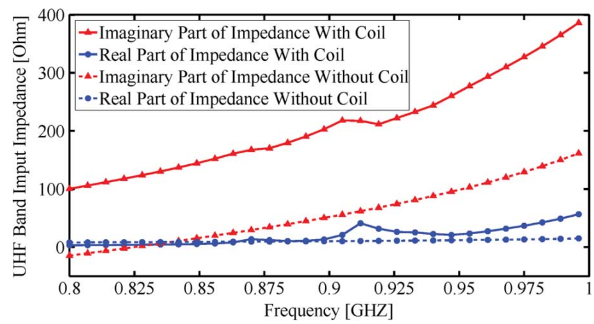

Fig. 4. Input impedance comparison with and without external coil.

their counterparts D_3 and D_4. Two rectangular slots in two arms are used to fine-tune the impedance. In the simulation and manufacture, we use FR4 ($\epsilon = 4.2$, $\tan\delta = 0.02$) substrate with the dimension of $85 \times 54 \times 0.8$ mm^3. Fig. 2 shows the manufactured antenna. The HF coil is designed for NXP Mifare ASIC that complies with the ISO/IEC 14443 standard. The UHF antenna operates with an Impinj Monza 3 Tag chip that has $32 - j216\ \Omega$ input impedance at 915 MHz and complies with the ISO 18000-6C standard. The typical values of read and write sensitivities for this chip are -15 and -11 dBm, respectively. This design is simulated and optimized in ANSYS HFSS.

III. Antenna Design and Analysis

A. HF Frequency Band

In the HF frequency band, the 13.56-MHz antenna operates as the near-field coupling antenna. The LC resonance relationship can be obtained by the microchip's impedance and external spiral coil. The resonance frequency is defined as $\omega_0 = 1/\sqrt{LC}$. The microchip's impedance is equivalent to a 17- pF capacitor. Hence, the external coil provides needed inductance. The suitable equivalent inductor of resonance can be achieved by adjusting the line width t_1, line gap distance D, length L_c, and width W_c of the whole coil.

In practical applications, because the tag will be placed on the reader during the reading process, extra coupling capacitances will be generated by contact. Hence, the resonance frequency without contact should be designed to a little higher frequency than the operating frequency (13.56 MHz). In [5], the authors set the frequency at 16.4 MHz. The band from 14.5 to 18.5 MHz is an acceptable range.

Fig. 3 shows the measured and simulated HF band input impedance. In the simulation, we adjust the coil's parameters to set the input impedance to $2.4 + j544\ \Omega$ at 13.56 MHz. Combined with the 17-pF equivalent capacitor, the calculated resonance frequency without reader contact is 15.28 MHz. From the measured result, at 13.56 MHz, the impedance is $5.4 + 519.8\ \Omega$. This result is very close to the simulated result.

B. UHF Frequency Band

The UHF antenna design is mainly focused on solving the narrowband issue under large inductance and high quality factor circumstances. Fig. 4 shows the input impedance comparison with and without an external coil. It is obvious that the external coil increases the inductor of the UHF antenna.

The original design intention is to use two dipoles to form two adjacent resonance frequencies to broaden the bandwidth, like the structure proposed in [9]. The best expectation is that the two dominant resonance modes could operate independently and have minimum mutual influences. The actual operating condition is more complex. Due to the limitation of compact size, we expect to build up a structure that has multiple potential modes, and then try to excite two of them through some simple adjustments. To add more adjustment capability and ensure multiple modes, this structure is proposed. The diagonal meander lines' dimensions are identical, and each two opposite meander lines parallel along the y-axis are different in dimensions. This ensures multiple resonance modes.

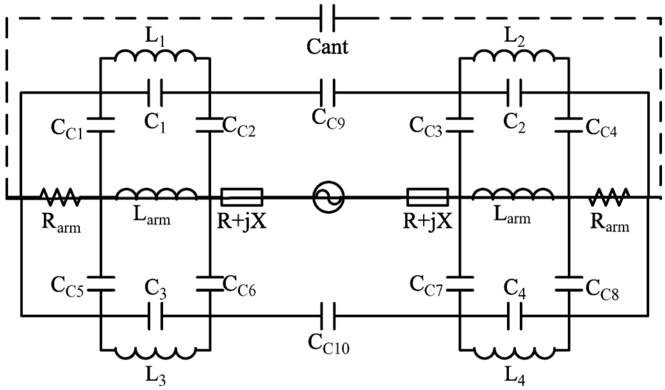

Fig. 5. Equivalent circuit of the design at the UHF band.

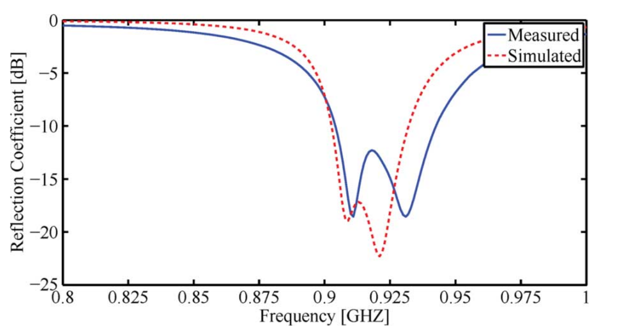

Fig. 6. Simulated and measured reflection coefficient of the antenna at the UHF band.

According to the antenna design, the equivalent circuit model is given in Fig. 5. In this figure, $R + jX$ is the equivalent component of the rectangle slot, and $C_{\rm Cant}$ is the antenna coupling capacitors. L_1–L_4, C_1–C_4, $R_{\rm arm}$, and $L_{\rm arm}$ represent four meander lines and two main patches' equivalent components, respectively. Among them, $C_{\rm Cant}$ connected by dashed lines is the dipole coupling capacitor. From the structure and its equivalent circuit model, it is easy to excite multiple resonance modes in this antenna. By adjusting four meander lines' dimensions, two adjacent resonance modes around 915 MHz can be easily obtained.

Fig. 6 shows the simulated and measured reflection coefficient. From the comparison, the simulated and measured data appear to be in a good agreement. Two obvious resonance peaks can be observed. The bandwidth is thereby broadened. In simulation, two resonance frequencies appear at 910 and 920 MHz, respectively. The bandwidth is around 30 MHz. The measured two resonance frequencies are at 911 and 931 MHz, respectively. The bandwidth is around 40 MHz broader than the simulation. It should be noted that all the reflection coefficients in this letter are calculated with respect to the chip impedance. We define the following equation in HFSS to do the calculation:

$$\Gamma = 20 * \log_{10}\left(\frac{Z_{\rm ant} - Z_{\rm chip}^{*}}{Z_{\rm ant} + Z_{\rm chip}}\right)$$

where Γ is the reflection coefficient, and $Z_{\rm ant}$ and $Z_{\rm chip}$ are impedances of the antenna and chip, respectively.

According to the reflection coefficient result, the simulated radiation patterns of xz- and yz-planes (corresponding to the coordinate presented in Fig. 1) are plotted in Fig. 7 at 910 and 920 MHz, respectively. The maximum gains are -5.36 and -1.89 dB at 910 and 920 MHz, respectively. Fig. 8 shows simulated frequency characteristic of the gain. To further analyze the UHF two working modes, the surface current distribution plots under two working modes (910 and 920 MHz) are given in Fig. 9.

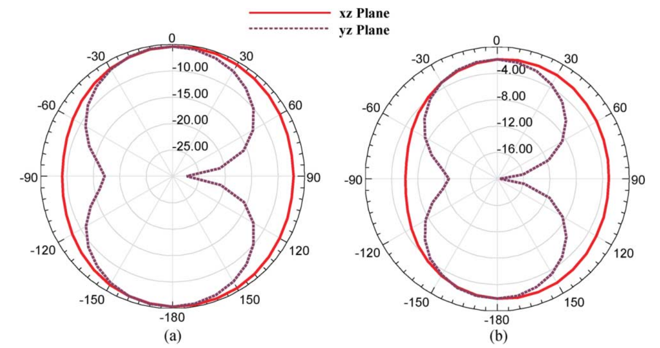

Fig. 7. Radiation patterns of xz-plane and yz-plane at (a) 910 and (b) 920 MHz.

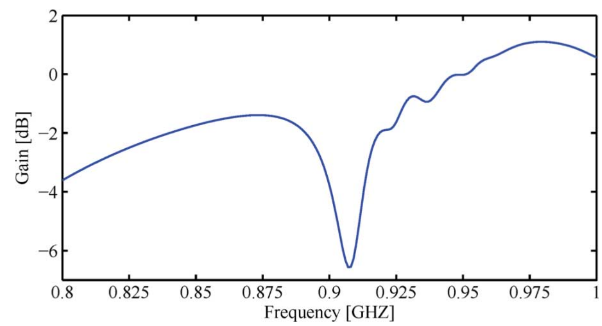

Fig. 8. Simulated frequency characteristic of the gain.

To understand the practical performance of the antenna, we measured the UHF antenna's reading range. Fig. 10 presents the measurement result. It is conducted with effective radiated power (ERP) 3.28 W and reader sensitivity -74 dBm. The reader is linearly polarized. The maximum reading range is 6.8 m and appears at 885 MHz. Another peak range is 4.4 m at 925 MHz. Nonlinear input impedance of the microchip may be the reason causing this resonance frequency shift. Due to the in-band dual resonance feature, there is a less-matching frequency in between two primary matching frequencies. Due to the nonlinearity of the chip impedance and some uncertainty parameters not considered in the simulation, the less-matching frequency point is shifted up a little bit to 920 MHz. It results in the low gain at that point.

C. Impedance Matching

For single-dipole applications, we have many methods to match the impedance, like T-match, loop coupling, and so on [10]. In this design, we expand the width of the main arm patches to conduct the coarse tuning and use rectangle slots to conduct the fine tuning. Fig. 11 shows the variation of reflection coefficient changing with M_1 from 6 to 8 mm. M_1's variation changes the coupling capacitors $C_{\rm C1}$ to $C_{\rm C8}$. Hence, the resonance frequencies have corresponding changes. The two slots on the main arm patches are equivalent to adding extra serial impedances to the antenna. The impacts of two slots are presented in Figs. 12 and 13. From these two figures, we find when the slots' dimensions are $A = B = 6$ mm, the

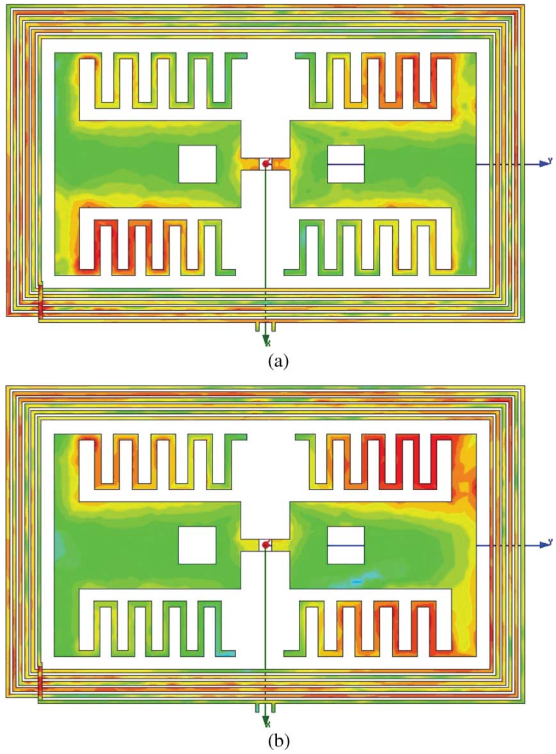

Fig. 9. Surface current distribution plots at (a) 910 and (b) 920 MHz.

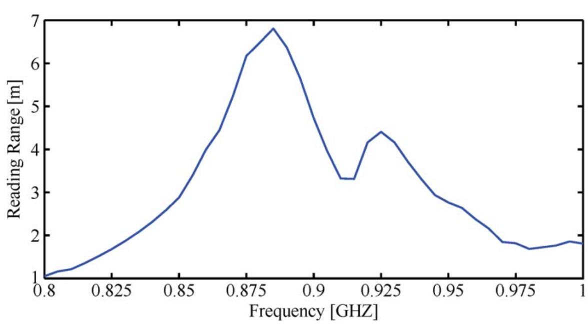

Fig. 10. Measured reading range.

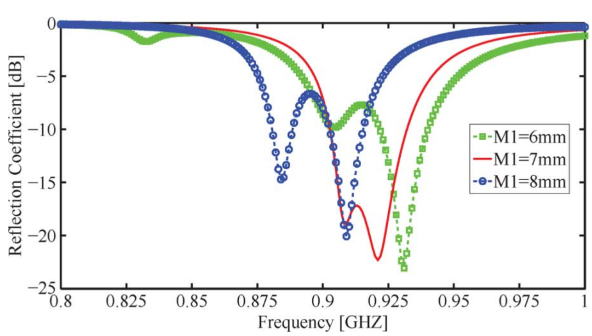

Fig. 11. Reflection coefficient for various main arm patches width M_1.

reflection coefficient curve is relatively smoothened and the difference between two peaks is minimum.

IV. Conclusion

This letter presents a novel single-layer compact RFID tag antenna, which operates in the HF (13.56 MHz) and UHF

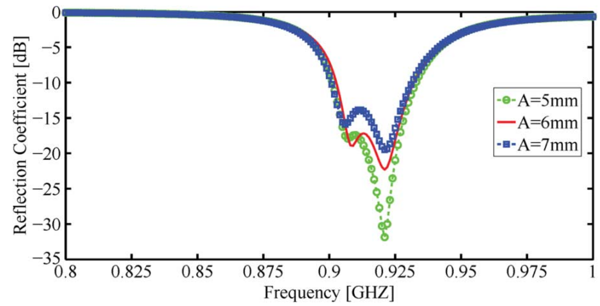

Fig. 12. Reflection coefficient for various slot width A.

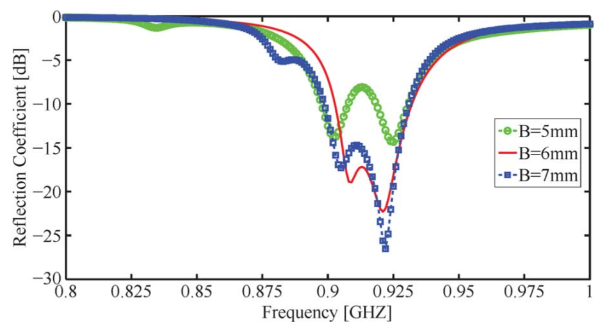

Fig. 13. Reflection coefficient for various slot length B.

(915 MHz) bands. It features the credit card compact size, low cost, and easy fabrication. Both operation principles in the HF and UHF band are analyzed and discussed. It solves the narrowband issue under the large inductive circumstance by using two adjacent UHF resonance modes. For the impedance matching, the methods of coarse tuning and fine tuning are also presented. Through practical manufacture and measurement, this antenna shows very good performance.

References

[1] G. Marrocco, "Gain-optimized self-resonant meander line antennas for RFID applications," *IEEE Antennas Wireless Propag. Lett.*, vol. 2, pp. 302–305, 2003.

[2] K. V. S. Rao, P. V. Nikitin, and S. F. Lam, "Antenna design for UHF RFID tags: A review and a practical application," *IEEE Trans. Antennas Propag.*, vol. 53, no. 12, pp. 3870–3876, Dec. 2005.

[3] T. Deleruyelle, P. Pannier, M. Egels, and E. Bergeret, "Dual band mono-chip HF-UHF tag antenna," in *Proc. IEEE Antennas Propag. Soc. Int. Symp.*, Toronto, Canada, Jul. 2010, pp. 1–4.

[4] A. Toccafondi, C. D. Giovampaola, F. Mariottini, and A. Cucini, "UHF-HF RFID integrated tag for moving vehicle identification," in *Proc. IEEE Antennas Propag. Soc. Int. Symp.*, Charleston, SC, Jun. 2009, pp. 1–4.

[5] P. Iliev, P. Le Thuc, C. Luxey, and R. Staraj, "Dual-band HF-UHF RFID tag antenna," *Electron. Lett.*, vol. 45, pp. 439–441, Apr. 2009.

[6] A. Toccafondil and P. Braconi, "Compact meander line antenna for HF-UHF tag integration," in *Proc. IEEE Antennas Propag. Soc. Int. Symp.*, Honolulu, HI, Jun. 2007, pp. 5483–5486.

[7] K. S. Leong, M. L. Ng, and P. H. Cole, "Miniaturization of dual frequency RFID antenna with high frequency ratio," in *Proc. IEEE Antennas Propag. Soc. Int. Symp.*, Honolulu, HI, Jun. 2007, pp. 5475–5478.

[8] Y. Nishioka, K. Hitomi, H. Okegawa, T. Mizuno, T. Fukasawa, H. Miyashita, and Y. Konishi, "Novel antenna configuration for HF- and UHF-band hybrid card-type RFID tags," in *Proc. 4th Eur. Conf. Antennas Propag.*, Apr. 2010, pp. 1–5.

[9] C. Cho, H. Choo, and I. Park, "Broadband RFID tag antenna with quasi-isotropic radiation pattern," *Electron. Lett.*, vol. 41, pp. 1091–1092, Sep. 2005.

[10] G. Marrocco, "The art of UHF RFID antenna design: Impedance-matching and size-reduction techniques," *IEEE Antennas Propag. Mag.*, vol. 50, no. 1, pp. 66–79, Feb. 2008.